# CrystEngComm

www.rsc.org/crystengcomm

Volume 15 | Number 47 | 21 December 2013 | Pages 10145–10406


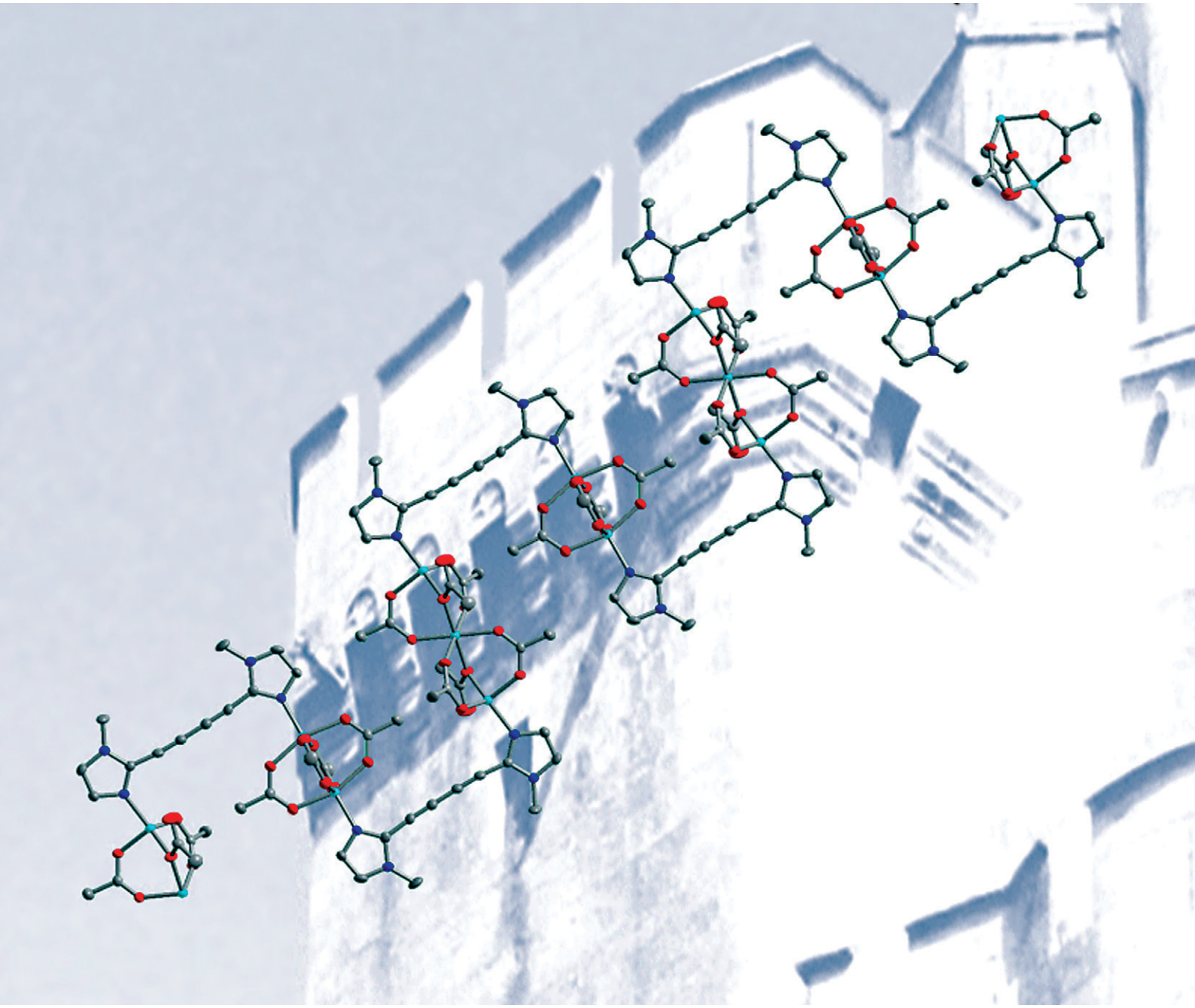


RSC Publishing


**COVER ARTICLE**

Guldi, Burzlaff *et al.*

Battlement-shaped 1D coordination polymer based on a bis(*N*-methylimidazole-2-yl)butadiyne ligand

CrystEngComm

RSC Publishing

COMMUNICATION

View Article Online
View Journal | View Issue



Cite this: *CrystEngComm*, 2013, **15**, 10157

Received 12th July 2013,
Accepted 21st August 2013

DOI: 10.1039/c3ce41652f

www.rsc.org/crystengcomm

# Battlement-shaped 1D coordination polymer based on a bis(*N*-methylimidazole-2-yl)butadiyne ligand†

Thomas Waidmann,[a] Nico Fritsch,[a] Johannes Tucher,[a] Marc Rudolf,[b] Felix Glaser,[a] Dirk M. Guldi*[b] and Nicolai Burzlaff*[a]

**Bis(*N*-methylimidazole-2-yl)butadiyne (bmib) has been prepared starting from *N*-methylimidazole following two different pathways. Bmib fluoresces and is capable of forming 1D coordination polymers by clamping together metal units. The molecular structure of a zinc coordination polymer based on bmib and zinc acetate resembles a battlement of a fortress.**

Unsaturated organic ligands in combination with transition metals can be used as precursors for inorganic–organic materials. These materials, based on their architecture and characteristics, are of great interest regarding catalysis, nonlinear optics, or properties that may be useful in electronic applications or as molecular sensors.[1] Molecular self-assembly is at the heart of crystal engineering and is based on complementary and explicit interactions between the components in order to generate the final product.[2] Two new branches excelled in this still emerging field, namely metal–organic coordination networks (MOCNs) or metal–organic frameworks (MOFs) and supramolecular coordination complexes (SSCs).[3] Synthesis of highly ordered coordination polymers can lead to molecular networks with different dimensions, *e.g.* linear polymers or "zigzag" chains and 2D planar or 3D polymer networks.[1–4] Our special interest focuses on the synthesis of new appropriate organic *N*,*N*-ligands suitable for 1D coordination polymers.[2a,b,5] In recent years, polyyne-bridged heterocycles, such as bis(4-pyridyl)butadiyne, have been proven to be powerful ligands for chain and square-grid architectures.[6] Recently, we reported on *trans*-1,2-bis(*N*-methylimidazole-2-yl)ethylene(*trans*-bie) which turned out to be a versatile building block for 2D and especially 1D coordination polymers.[7] Inspired by the results gained, we decided to aim for the new linear bis(*N*-methylimidazole-2-yl)butadiyne (bmib) (**7**).

The first approach to get hands on the bmib ligand started with 1-methylimidazole-2-carbaldehyde (**2**) that is accessible from 1-methylimidazole (**1**) (Scheme 1).[8] A Wittig reaction of **2** and chloromethylene-(triphenyl)phosphine resulted in 2-(2'-chlorovinyl)-*N*-methylimidazole that was obtained as a 2 : 1 mixture of *E*/*Z* isomers **3a/b**. Treating 2-(2'-chlorovinyl)-*N*-methylimidazole (**3a/b**) with potassium *tert*-butoxide yielded the 2-ethynyl-*N*-methylimidazole (**6**) suitable for a Glaser coupling. Due to a rather cumbersome purification of **3a/b**, mostly caused by unreacted Wittig reagent, we decided to follow another route to 2-ethynyl-*N*-methylimidazole (**6**). This second approach involved 2-iodo-1-methylimidazole (**4**) which is gained by a reaction of 1-methylimidazole (**1**) with *n*-butyl lithium and $I_2$.[9] The resulting imidazole **4** was treated under Sonogashira coupling conditions to yield 2-trimethylsilyethynyl-1-methylimidazole (**5**).[10] After desilylation with KF, bis(*N*-methylimidazole-2-yl)butadiyne (bmib) (**7**) was obtained by a homocoupling Glaser reaction of **6** catalyzed by CuCl in pyridine (Scheme 1).

Bmib (**7**) crystallizes in the space group $P2_1/c$, and the result of an X-ray single crystal structure determination shows the presence of intermolecular π-stacking (Fig. 1). The average distance between the centres of the stacking imidazoles is approximately 3.6–3.7 Å. Bond distances of the acetylene chain show prevalent values with a triple bond distance of 1.202 Å.[6a,11]

Similar to related compounds,[12] the absorption spectrum (Fig. 2) of bmib (**7**) gives rise to vibronic transitions in the 280 to 350 nm range with maxima at 292, 308, 328, and 350 nm with an energetic spacing of 2000 $cm^{-1}$. These are assigned to the triple bond centered π–π* excited state. Following excitation at a wavelength of 300 nm, an emission spectrum that gives

[a] *Department of Chemistry and Pharmacy, University of Erlangen-Nürnberg, Egerlandstrasse 1, 91058 Erlangen, Germany. E-mail: nicolai.burzlaff@fau.de; Fax: +49 9131 85 27387; Tel: +49 9131 85 28976*

[b] *Department of Chemistry and Pharmacy, University of Erlangen-Nürnberg, Egerlandstrasse 3, 91058 Erlangen, Germany. E-mail: dirk.guldi@fau.de; Fax: +49 9131 85 27341; Tel: +49 9131 85 28307*

† Electronic supplementary information (ESI) available: Experimental details for synthesis and characterization details, crystallographic data for **7** & **8**. CCDC 949213–949214. For ESI and crystallographic data in CIF or other electronic format see DOI: 10.1039/c3ce41652f

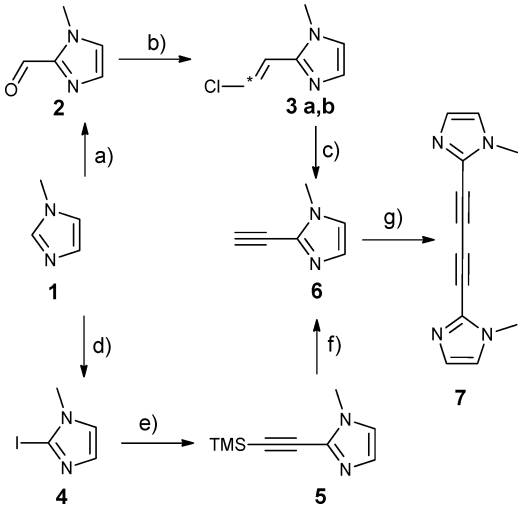


**Scheme 1** Synthesis of bmib *via* two different pathways. (a) *n*-BuLi, DMF, THF. (b) *n*-BuLi, (chloromethyl)triphenylphosphonium chloride, THF. (c) KO$^t$Bu, $NH_4Cl$, THF. (d) *n*-BuLi, $I_2$, THF. (e) $Pd(PPh_3)_2Cl_2$, CuI, $Et_3N$, DMF, TMS-acetylene. (f) KF, MeOH. (g) CuCl, $O_2$, pyridine.

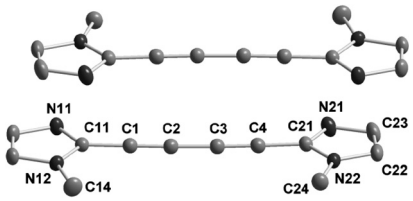


**Fig. 1** The molecular structure of bmib (**7**); thermal ellipsoids are drawn at the 30% probability level, and hydrogen atoms have been omitted for clarity. Selected bond lengths (Å) and angles (°): C3–C2, 1.366(19); C2–C1, 1.202(19); C1–C11, 1.417(18); C14–N12, 1.454(17); C2–C1–C11, 179.05(14); C3–C2–C1, 178.35(14); N11–C11–C21–N21, 178.04(14).

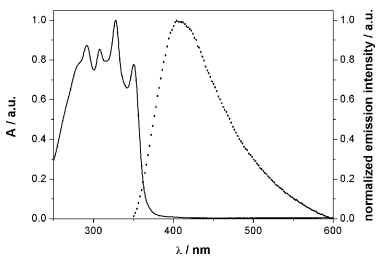


**Fig. 2** The absorption (solid line) and emission (dotted line) spectra for bmib (**7**) in $CHCl_3$ at 300 nm excitation wavelength.

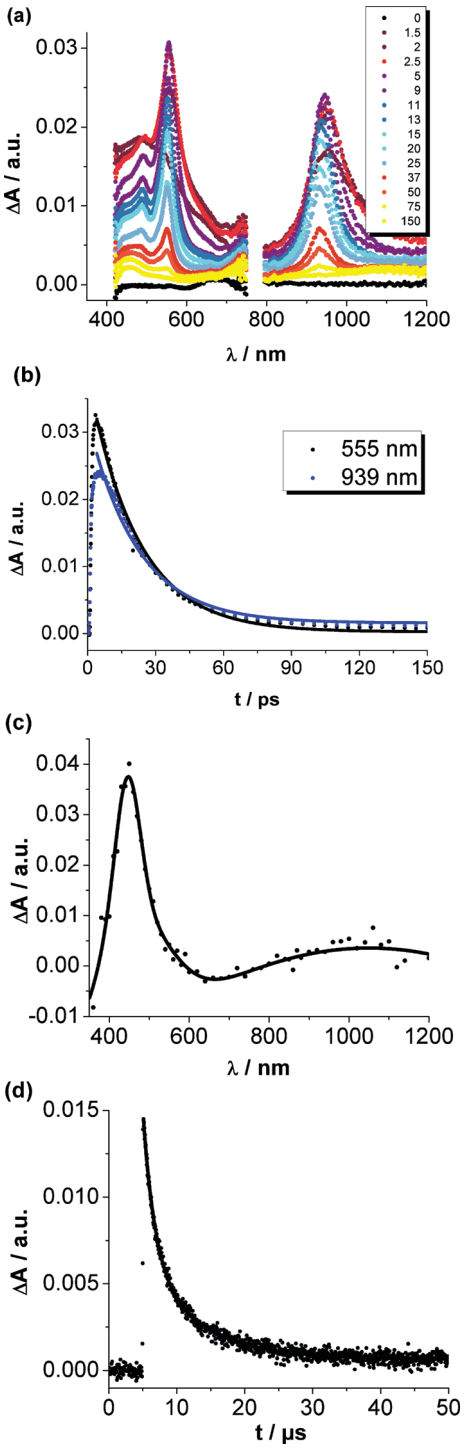


**Fig. 3** (a) Differential absorption spectra (visible and near-infrared) obtained upon femtosecond pump probe experiments (258 nm) of bmib (**7**) in argon-saturated THF with several time delays between 0 and 150 ps at room temperature. (b) Time–absorption profiles of the spectra shown in (a) at 555 and 939 nm, monitoring the intersystem crossing. (c) Differential absorption spectra (visible and near-infrared) obtained upon nanosecond flash photolysis (266 nm) of bmib (**7**) in argon-saturated THF at 50 ns after excitation at room temperature. (d) Time–absorption profile of the spectrum shown in (c) at 450 nm, monitoring the excited state decay.

rise to a 115 nm red-shifted maximum at 415 nm evolves. Emission quantum yields were as high as $1.5 \times 10^{-3}$ and $1.1 \times 10^{-3}$ in $CHCl_3$ and THF, respectively.

Further insights into the excited state deactivation of bmib (7) came from transient absorption measurements following femtosecond and nanosecond excitation in THF (Fig. 3, top). Upon 258 nm excitation, we note intense transient absorption features throughout the visible and near-infrared region, which maximize at 490, 555, and 939 nm. We interpret these differential absorption changes as the population of the singlet excited state of bmib (7). On a rather short timescale,

 

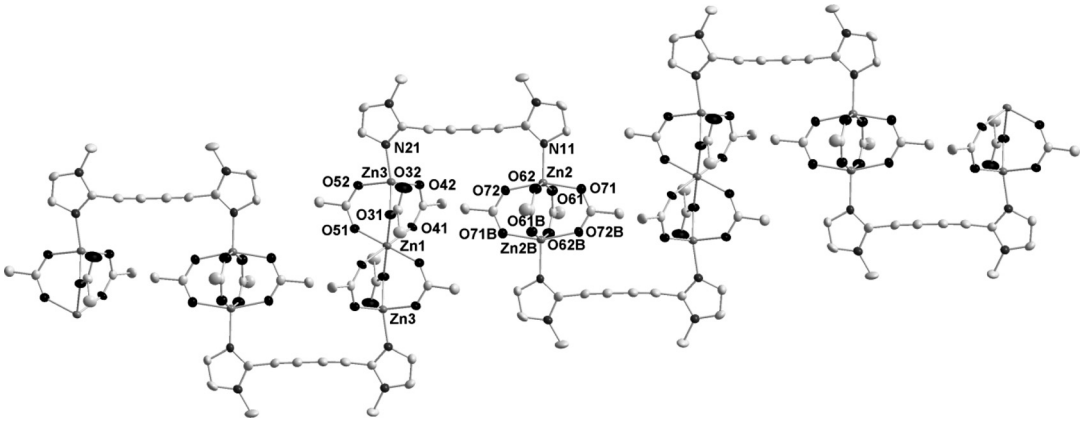


**Fig. 4** Battlement arrangement of coordination polymer **8**.

that is, 25 ± 5 ps, these transient absorption features decay. At the end of this decay, we note a broad transient absorption throughout the visible and near-infrared region with maxima at 450 and around 1100 nm. The latter are stable and are still discernible at the end of the experimental timescale of 7.5 ns. Tentatively, we ascribe these transients to the triplet excited state of bmib (7). To explore the triplet excited state deactivation, nanosecond transient absorption measurements with 266 nm laser pulses were performed (Fig. 3, bottom). The nanosecond transient absorption spectrum is in perfect agreement with what was observed at the end of our femtosecond transient absorption measurements. In particular, transient absorption features with maxima at 450 and around 1100 nm were noted. A kinetic analysis revealed two lifetimes—a short-lived component with 1.7 ± 0.2 and a long-lived component with 7.9 ± 0.5 μs. The two components are likely to arise from triplet–triplet annihilation and ground-state quenching. Support for the assignment that the transient features correlate with the triplet excited state of bmib (7) came from analogous experiments in oxygen-saturated solutions. In the latter, the triplet excited lifetime is reduced to 80 ± 5 ns.

Reaction of bmib with $Zn(OAc)_2$ yielded a 1D polymeric compound. The X-ray structure analysis revealed coordination polymer $[Zn_5(OAc)_{10}(bmib)_2]_n$ consisting of alternating dinuclear $[Zn_2(O_2CCH_3)_4]$ paddle-wheel units and trinuclear $[Zn_3(O_2CCH_3)_6]$ units "clamped" together by bmib ligands. This rather unusual coordination mode of the bmib ligand causes a one-dimensional sequence that resembles a battlement of a fortress (Fig. 4). Zinc acetate is capable of forming coordination polymers with *N*,*N*-donor ligands by either having a paddle-wheel or trinuclear inorganic unit.[13–16,18] To the best of our knowledge, such alternating paddle-wheel and trinuclear units have been reported only once in literature before.[19]

The trinuclear Zn(II) acetate unit is constructed by six bridging acetate ligands and similar to previously described trinuclear zinc carboxylates with axial *N*- or *O*-donor ligands.[13–16] There is an inversion centre on the central Zn atom. Out of three Zn atoms, the central Zn is all *O*-donor hexacoordinated from six acetate groups to form a distorted octahedron. The two terminal Zn centres are coordinated tetrahedrally by three oxygen atoms of the acetate groups and by the nitrogen atom of the bmib ligand. Two different types of carboxylate coordination were found in this unit. Four acetate ligands show $\kappa^2$-coordination, forming *syn–syn* bridges between central and terminal zinc ions. The other two acetate ligands are $\kappa^1$-coordinated and function as Zn–O–Zn μ-bridges with one uncoordinated oxygen atom slightly involved in a weak interaction with the zinc atom ($d$(Zn3···O32) = 2.645(4) Å).[17] The paddle-wheel unit is constructed by two symmetrically equivalent Zn atoms, which are μ-bridged by four acetate ligands. Each Zn atom in this unit is in a distorted square pyramidal environment, with four oxygen atoms from acetates, to form the equatorial plane, and one nitrogen atom of the bmib ligand. In the paddle-wheel unit, the Zn–O bond distances range from 2.035(3) to 2.077(4) Å and the Zn–N bond distance amounts to 2.034(4), which compare well to values of related compounds.[13,18] In the trinuclear unit, the Zn–O bond distances of the $\kappa^2$-OAc range from 1.938(4) to 2.118(3) Å. The $\kappa^1$-OAc shows a bond distance of 2.129(3) for Zn1–O31 and 1.980(3) for Zn3–O31. The Zn–N bond distance of 2.002(4) Å is slightly shorter than in the dinuclear unit. The Zn–Zn distances of dinuclear and trinuclear units are 2.9489(10) and 3.3287(6) Å, which are similar to literature values.[20] The bond distances of the bmib ligand do not vary significantly from those of the free ligand. It is worthwhile mentioning that obviously bmib (7) acts as some sort of molecular clip for metal ions with almost fixed angles ∠(M–N11–N21) close to 90° and torsion angles ∠(M–N11–N21–M') close to 0°. A similar coordination property has recently been reported for the slightly shorter 1,4-bis(*N*-methylimidazole-2-yl)benzene ligand.[20]

## Conclusion

The ligand 1,4-bis(*N*-methylimidazole-2-yl)butadiyne (bmib) (7) shows fluorescent properties in solution and intermolecular π-stacking in the crystal structure. Bmib (7) possesses remarkable coordination properties, as is indicated by the formation of a coordination polymer $[Zn_5(OAc)_{10}(bmib)_2]_n$ (**8**). The X-ray diffraction revealed an interesting battlement-type structure

with alternating trinuclear and dinuclear paddle-wheel zinc acetate units clamped together by bmib (7). The metal–bmib–metal units resemble the geometry of retaining clips.

## Acknowledgements

This work was supported by "Solar Technologies go Hybrid"—an initiative of the Bavarian State Ministry for Science, Research and Art.



## Notes and references

1 (*a*) K. Birahanda, M. Sarkar and L. Rajput, *Chem. Commun.*, 2006, 4169; (*b*) L. Brammer, *Chem. Soc. Rev.*, 2004, **33**, 476.
2 (*a*) A. Robin and K. Fromm, *Coord. Chem. Rev.*, 2006, **250**, 2127; (*b*) A. N. Khlobystov, A. J. Blake, N. R. Champness, D. A. Lemenovskii, A. G. Majouga, N. V. Zyk and M. Schröder, *Coord. Chem. Rev.*, 2001, **222**, 155; (*c*) C. B. Aakeröy, N. R. Champness and C. Janiak, *CrystEngComm*, 2010, **12**, 22.
3 (*a*) T. R. Cook, Y.-R. Zheng and P. Stang, *Chem. Rev.*, 2013, **113**, 734; (*b*) R. Chakrabarty, P. S. Mukherjee and P. Stang, *Chem. Rev.*, 2011, **111**, 6810; (*c*) C. Janiak, *Dalton Trans.*, 2003, 2781.
4 (*a*) S. L. James, *Chem. Soc. Rev.*, 2003, **32**, 276; (*b*) A. J. Blake, N. R. Champness, P. Hubberstey, W.-S. Li, M. A. Withersby and M. Schröder, *Coord. Chem. Rev.*, 1999, **183**, 117; (*c*) O.-S. Jung, Y. J. Kim, Y.-A. Lee, J. K. Park and H. K. Chae, *J. Am. Chem. Soc.*, 2000, **122**, 9921; (*d*) R. J. Hill, D.-L. Long, N. R. Champness, P. Hubberstey and M. Schröder, *Acc. Chem. Res.*, 2005, **38**, 337.
5 R. Mas-Ballesté, O. Castillo, P. J. Sanz Miguel, D. Olea, J. Gómez-Herrero and F. Zamora, *Eur. J. Inorg. Chem.*, 2009, 2885.
6 (*a*) J. R. Allan, M. J. Barrow, P. C. Beaumont, L. A. Macindoe, G. H. W. Milburn and A. R. Wernick, *Inorg. Chim. Acta*, 1988, **148**, 85; (*b*) M. Maekawa, H. Konaka, Y. Suenaga, T. Kuroda-Sowa and M. Munakata, *J. Chem. Soc., Dalton Trans.*, 2000, 4160; (*c*) M. B. Zaman, M. D. Smith and H.-C. zur Loye, *Chem. Mater.*, 2001, **13**, 3534; (*d*) A. Haim, *Inorg. Chem.*, 1983, **30**, 273; (*e*) M. B. Zaman, K. A. Udachin and J. A. Ripmeester, *CrystEngComm*, 2002, **4**(103), 613; (*f*) J. Atienza, A. Gutiérrez, M. Felisa Perpinán and A. E. Sánchez, *Eur. J. Inorg. Chem.*, 2008, 5524.
7 N. V. Fischer, M. S. Alam, I. Inshad Jumh, M. Stocker, N. Fritsch, V. Dremov, F. W. Heinemann, N. Burzlaff and P. Müller, *Chem.–Eur. J.*, 2011, **17**, 9293.
8 J. G. Rodríguez and C. Díaz-Oliva, *Tetrahedron*, 2009, **65**, 2512.
9 A. S. Bhanu Prasad, T. M Steveson, J. R. Citineni, V. Nyzam and P. Knoche, *Tetrahedron*, 1997, **53**, 7237.
10 A. Satake, O. Shoji and Y. Kobuke, *J. Organomet. Chem.*, 2007, **692**, 635.
11 S. M. Curtis, N. Le, F. W. Fowler and J. W. Lauher, *Cryst. Growth Des.*, 2005, **5**(6), 2313.
12 K. Zhang, J. Hu, K. C. Cha, K. Y. Wong and J. H. K. Yip, *Eur. J. Inorg. Chem.*, 2007, 384.
13 H. Kwak, S. H. Lee, S. H. Kim, Y. M. Lee, B. K. Park, E. Y. Lee, Y. J. Lee, C. Kim, S.-J. Kim and Y. Kim, *Polyhedron*, 2008, **27**, 3484.
14 A. Karmaker, R. J. Sarma and J. B. Baruah, *Inorg. Chem. Commun.*, 2006, **9**, 1169.
15 W. Clegg, I. R. Little and B. P. Straughan, *Inorg. Chem.*, 1988, **27**, 1916.
16 C. A. Williams, A. J. Blake, P. Chem and M. Schröder, *Chem. Commun.*, 2005, 5435.
17 V. Zeleňák, M. Sabo, W. Massa and P. Llewellyn, *Inorg. Chim. Acta*, 2004, **357**, 2049.
18 (*a*) B. Singh, J. R. Long, F. F. de Biani, D. Gattesch and P. Stavropoulos, *J. Am. Chem. Soc.*, 1997, **119**, 7030; (*b*) W. Clegg, I. R. Little and B. P. Straughan, *J. Chem. Soc., Dalton Trans.*, 1986, 1283; (*c*) H. Li, M. Eddaoudi, T. L. Groy and O. M. Yaghi, *J. Am. Chem. Soc.*, 1998, **120**, 8571–8572; (*d*) H. Chun and J. Moon, *Inorg. Chem.*, 2007, **46**, 4371.
19 H. Kwak, S. H. Lee, S. H. Kim, Y. M. Lee, B. K. Park, Y. J. Lee, J. Y. Jun, C. Kim, S.-J. Kim and Y. Kim, *Polyhedron*, 2009, **28**, 553.
20 S. Pal, W.-S. Hwang, I. J. B. Lin and C.-S. Lee, *J. Mol. Catal. A: Chem.*, 2007, **269**, 197.

 